Theor Appl Climatol (2011) 106:307–319
DOI 10.1007/s00704-011-0427-7

ORIGINAL PAPER

The impact of El Niño on South American summer climate during different phases of the Pacific Decadal Oscillation

Gyrlene Aparecida Mendes da Silva · Anita Drumond · Tércio Ambrizzi

Received: 18 February 2010 / Accepted: 23 February 2011 / Published online: 9 April 2011

Abstract In austral summer, the observed El Niño (EN) events during warm Pacific Decadal Oscillation (PDO) phases (PDO(+)) exhibited large anomalous upper level wave patterns in response to larger Sea Surface Temperature (SST) anomalies in the Equatorial Pacific and Atlantic Oceans compared with SST anomalies in EN events during cold PDO phases (PDO(−)). The precipitation anomalies in PDO(+) EN are increased over Southeastern South America (SESA) associated with the intensification of the moisture flux convergence in this region. The PDO(−) EN events exhibit positive precipitation anomalies only over southern SESA, while negative anomalies were observed in the north. Downward motion and anomalous divergence over central eastern Brazil may have contributed to the weakening of the northwesterly moisture flux convergence associated with the South American Low Level Jet (SALLJ) over the subtropics. The extratropical cyclones showed higher frequency and lower central pressures in southern Brazil, Uruguay, northeastern Argentina, and Southwest Atlantic Ocean during the PDO(+) EN events compared with the PDO(−) EN events. Such increase in the frequency and intensity of cyclogenesis cases seems to be in accordance with the anomalous moisture flux convergence over the SESA and associated reduction in the Sea Level Pressure observed during PDO(+) EN events. In order to investigate the impact of a canonical El Niño event over South America under different PDO phases, two numerical experiments were done with an Atmospheric General Circulation Model. Global SST and ice sea fields average over years characterized by (a) PDO(+) and (b) PDO(−) were considered as climatologically fields, and a composite of anomalies of SST of all El Niño events observed in 1950–1999 was added in the region 20ºS–20ºN;120ºW–175ºW of both "climatologies." The differences in experiments suggest that a canonical EN may produce significant different anomalous atmospheric patterns associated with distinct PDO climatologies. The more significant differences are simulated over extreme northern and eastern Brazil. Additional numerical experiments isolating the observed variability of SST over several oceanic basins during different PDO phases will be conducted to study their particular role on the South American climate.

G. A. M. Silva (✉) · T. Ambrizzi
Department of Atmospheric Sciences, Institute of Astronomy, Geophysics and Atmospheric Sciences, University of São Paulo, Rua do Matão, 1226, Cidade Universitária, São Paulo, SP 05508-090, Brazil
e-mail: gyrlene@model.iag.usp.br

A. Drumond
EPhysLab, Facultade de Ciencias, Universidad de Vigo, Ourense, Spain

1 Introduction

Several observational studies have extensively documented ENSO-related precipitation anomalies over the globe and their apparent modulation by the Pacific Decadal Oscillation (PDO). Mantua et al. (1997), for example, describes the PDO as the first mode obtained via Empirical Orthogonal Function (EOF) analysis of the monthly SST anomalies observed in the North Pacific during the period between 1900 and 1993. Power et al. (1999) and Folland et al. (2002) pointed out that interdecadal variability in the PDO time series is very similar to the evolution of the Interdecadal Pacific Oscillation (IPO), which is a Pacific basin-wide ENSO-like pattern of variability. The warm phase, PDO(+) or El Niño-like phase of the PDO and IPO, exhibits an anomalously deep Aleutian low-pressure system, colder

surface waters in the western and central North Pacific, and warmer SST along the west coast of Americas and in the central and eastern tropical Pacific (e.g., Mantua et al. 1997; Enfield and Mestas-Nuñez 1999). The cold phase, PDO(−) or La Niña-like phase, features reversed patterns. Moreover, the anomalous SST pattern related to the PDO and IPO is nearly symmetric about the equator, but is less equatorially confined in the eastern Pacific than the ENSO mode (Zhang et al. 1997; Power and Colman 2006).

While the impact of the PDO and IPO on ENSO teleconnections to Australia (Power et al. 2006), the North Pacific (Newman et al. 2003), and South Pacific (Power and Colman 2006) has been studied, much less attention has been given to the response over South America. Robertson and Mechoso (2000) have found an increase on precipitation and river flow over southeastern continent and southeastern Amazon region, and a decrease over northern Amazon (Marengo 2004) after 1976/77 consistent with the mode phase change. However, this cannot be exclusively attributed to the PDO variability, because the EN events have been more intense and frequent in the 1980s and 1990s decades (Ambrizzi et al. 2004), and the frequency of LN events was low during this period (Power and Smith 2007). Dettinger et al. (2001) suggest that despite potentially different source mechanisms, both interannual and decadal ENSO-like climate variations yield wetter subtropics (when the ENSO-like indices are in positive) and drier midlatitudes and tropics over the Americas, in response to equatorward shifts in westerly winds and storm tracks in both hemispheres.

Recent studies by Andreoli and Kayano (2005), Garcia and Kayano (2006), and Kayano and Andreoli (2007) are relevant here. Andreoli and Kayano (2005) verified that the EN signal on the Southern American precipitation during January and February is more pronounced during PDO(+) compared to the PDO(−). On the other hand, Kayano and Andreoli (2007) found that between November and April, the differences on the intensities of the ENSO teleconnection increase (decreases) when ENSO and PDO are in the same (opposite) phase. Also, the impact of the PDO on extratropical cyclones over the South Hemisphere has been explored by Schneider (2005) and Pezza et al. (2007). Pezza et al. (2007) suggested that during austral summer, the Sea Level Pressure (SLP) composite shows a strong annular structure related to the PDO, which is not seen for the ENSO index, with lower pressure around Antarctica during the positive phase and vice versa. More intense and fewer cyclones and anticyclones were observed during the positive PDO. This is less consistent for the ENSO index, particularly during the summer when a different PDO/ENSO pattern arises at high latitudes.

A detailed investigation of the dynamical variability of the South American Low Level Jet (SALLJ) and properties of extratropical cyclones over the South American continent in response to EN events observed during PDO(+) and PDO(−) phase was not explored in the previous observational studies. So, the main purpose of the present study is to investigate possible differences in the austral summer atmospheric circulation over South America during EN events observed in different PDO phases. Complementing our observational analysis, numerical experiments with an Atmospheric General Circulation Model (AGCM) will be conducted to investigate whether different phases of the PDO may affect the canonical EN teleconnections toward South America.

The data and methodology used are described in Section 2. An observational analysis of the anomalous climatic patterns and extratropical cyclone properties related to EN years during opposite PDO phases is described in Section 3.1. The results from the numerical experiments are described in Section 3.2, and the main findings are summarized in Section 4.

2 Data and methodology

2.1 Data

This study focuses on austral summer (December–January–February) between 1950 and 1999. This season was chosen because the Rossby wavelike response during EN years is amplified and more zonally symmetric in the Southern Hemisphere (Kiladis and Mo 1998). In addition, a more intense meridional moisture transport from the tropics to the subtropics due to the SALLJ occurs in this season (Paegle 1998; Douglas et al. 2000; Saulo et al. 2000; Marengo et al. 2004), and this mechanism is intensified in EN years (Silva and Ambrizzi 2006; Silva et al. 2009). Consequently, a more pronounced interaction between the tropical continental convection and the extratropical cyclones can be observed (Mendes et al. 2007).

Table 1 shows the EN extremes (strong and weak cases) and neutral ENSO selected according the classification of Zhou et al. (2001). Only extreme EN events were selected because they are associated with a higher variability of the amplitude of Equatorial Pacific SST anomalies. The classification of Zhou et al. (2001) uses the SST reanalysis produced at the National Centers for Environmental Production (NCEP/CPC, Smith et al. 1996) and the UK Meteorological Office (Parker et al. 1995). It is based on a key region over the equatorial Pacific (from 150°W to the date line). The selected EN events were then grouped according to the PDO index from Mantua et al. (1997).

The gridded precipitation data were obtained from Chen et al. (2002) on 2.5° regular horizontal resolution. Monthly mean streamfunction (ψ) at the 0.21 sigma level

Table 1 El Niño and neutral events selected according to the Oceanic Niño Index (ONI)/ NOAA criterion and separated according to warm and cold PDO phases

	El Niños	Neutral events
PDO(−)	1952/53, 1957/58, 1958/59, 1963/64, 1969/70, 1972/73	1951/52, 1953/54, 1956/57, 1959/60, 1960/61,1961/62, 1962/63,1966/67, 1967/68, 1971/72
PDO(+)	1976/77, 1977/78, 1979/80, 1982/83, 1987/88, 1990/91, 1991/92, 1992/93, 1994/95, 1997/98	1978/79, 1980/81, 1981/82, 1985/86, 1989/90, 1993/94, 1996/97

(corresponding to approximately 200 hPa) and HadSST1 datasets from the UK Meteorological Office Hadley Centre (Rayner et al. 2003) in a 2.0°×2.0° longitude–latitude grid were used. Monthly data from the NCEP/NCAR reanalysis (Kalnay et al. 1996) on a 2.5°×2.5° latitude–longitude grid are also used. The variables for the analysis are horizontal wind (u, v), specific humidity from 1,000 hPa up to 850 hPa, and vertical p-velocities (ω) at the 500 hPa level. In addition, six-hourly SLP reanalysis was used for the same period in order to apply an automatic tracking scheme (Murray and Simmonds 1991a, b).

2.2 Methodology

2.2.1 Observational study

A composite technique was used to calculate the EN-related anomalous patterns during the two distinct PDO regimes (positive, PDO(+), and negative, PDO(−)). The variables analyzed were precipitation, SST, 200 hPa zonally asymmetric streamfunction (ψ), and 500 hPa omega (ω). The vertically integrated moisture flux and its divergence between 1,000 and 850 hPa were also calculated as in Drumond and Ambrizzi (2005) and Silva and Ambrizzi (2009) to identify possible changes in the moisture transport and its convergence at low levels. Monthly anomalies of the variables are calculated as the differences between EN events minus the neutral years separately for each PDO phase. According to Silvestri (2004) and Vera et al. (2004), the climatology mean of neutral years may be the most appropriate method for exploring the signal of ENSO episodes because of the nonlinear relation between the equatorial Pacific SST forcing and the associated precipitation anomalies over some regions in South America. Although Table 1 contains a total 17 ENSO neutral years with 10 in the PDO(−) and 7 in the PDO(+), the differences between EN and neutral years are calculated separately for each PDO phase, as well the statistical significance of the anomalies, and the unbalanced number of neutral years in the PDO phases would not induce errors in the climatology.

An automatic tracking scheme identifies the cyclonic centers near the surface over the southern part of the continent, including the SESA domain. This tracking scheme, originally developed by Murray and Simmonds (1991a), has extensively been used in many studies over the Southern Hemisphere (Pezza and Ambrizzi 2003; Carvalho et al. 2005; Pezza et al. 2007; Reboita et al. 2009). More details on the scheme are given in Silva and Ambrizzi (2009) and references therein. The properties analyzed are the System Density (SD) and Central Pressure (CP). The SD is defined as the number of systems per unit area found in a region delimited by 5° latitude×5° longitude, and it is calculated by adding contributions from all sampled positions. The CP is defined as the average pressure at the center of each system inside this region. The analyses are made every 6 h because the scheme shows improvement in this time resolution (Pezza and Ambrizzi 2003; Pezza et al. 2007). The SLP equal to or below 1,010 hPa were considered, eliminating the weak systems related to cyclogenesis cases (Pezza and Ambrizzi 2003).

The results are based on the EN-related anomaly composites of SST, atmospheric circulation variables, and extratropical cyclones properties obtained for the two PDO regimes separately. A two-tailed Student's *t* test (Wilks 1995) was applied to the composites of anomalies to determine the areas where they are statistically significant at the 90% level. We consider that each event is independent representing 1° of freedom..

2.2.2 The AGCM numerical experiments

Two sensitivity experiments were performed with the purpose of investigating the impact of the canonical EN SST anomalies in the opposite PDO phases on atmospheric circulation over South America. The model used is the Community Atmosphere Model version 3.0 (CAM3) developed by the National Center for Atmospheric Research (NCAR), and it represents the atmospheric component of Community Climate System Model version 3.0. The formulation of the physics and dynamics is described in Collins et al. (2006). The version used here has 26 vertical levels and an 85-wave triangular spectral truncation (T85L26). The CAM3 was integrated in its standalone mode with specified SSTs and sea ice extent while coupled with the Community Land Model (CLM; Oleson et al. 2004). For more details, see Collins et al. (2006b).

Table 2 describes the sensitivity experiments using the AGCM CAM3 model. Monthly global SST and sea ice average conditions over years characterized by (a) PDO(+)

Table 2 Description of the numerical experiments using the AGCM CAM3 model

Experiment	Forcing in domain between 20ºS–20ºN;120ºW–175ºW	Climatology
ENPDO(+)	$aSST_{(El\ Niños1950\text{-}1999)} + mean\_SST_{(neu\_PDO(+))}$	$mean\_SST_{(neu\_PDO(+))}$ and $mean\_sea\ ice_{(neu\_PDO(+))}$
ENPDO(−)	$aSST_{(El\ Niños1950\text{-}1999)} + mean\_SST_{(neu\_PDO(-))}$	$mean\_SST_{(neu\_PDO(-))}$ and $mean\_sea\ ice_{(neu\_PDO(-))}$

and (b) PDO(−) were defined as "climatology fields." A composite of monthly anomalies of SST over 20ºS–20ºN;120ºW–175ºW for all El Niño events observed in 1950–1999 was considered as our "EN forcing" (EN SST) . This composite of anomalies is based on departures from ENSO neutral years observed during the period considered. So, in the ENPDO(+) experiment, the model is forced by EN SST composite anomaly in the Equatorial Pacific added to the global PDO(+) SST and sea ice climatologies. The ENPDO(−) experiment was forced with the same EN SST forcing, but considering monthly global climatologies of SST and sea ice related to the PDO(−) phase. The experiments were performed from September to March, and the period analyzed was from December to February. An ensemble of ten integrations was performed for each experiment, and the initial conditions were taken by specifying a random perturbation applied to the initial temperature field.

3 Results

3.1 Summertime South American atmospheric circulation, El Niño, and PDO: observational analysis

Figure 1 illustrates the composite of summertime precipitation and SST anomalies during EN years for the PDO(+) (Fig. 1a, b, respectively) and PDO(−) (Fig. 1c, d, respectively). Positive precipitation anomalies are observed over most part of the SESA, particularly over southern Brazil, Uruguay, southern Paraguay, and Central North Argentina during PDO(+) (Fig. 1a). Slightly negative anomalies predominate over the northern part of continent including the Amazon region between 0–10ºS. The SST composite exhibits anomalous warmer waters over equatorial Pacific between 180–80ºW with maximum values of approximately 1.6°C in 150–90ºW (Fig. 1b).

During EN years in the PDO(−) phase, negative precipitation anomalies were observed over the northern Amazon, but they were weaker than the ones observed in EN years during PDO(+) years (Fig. 1a, c, respectively). This result agrees with Marengo (2004), who found an increase in the magnitude of negative precipitation anomalies between 1975 and 1998 over this region associated with an increase in the frequency of the EN events and a reduction in the frequency of LN years. However, some caution needs to be considered as few observational data were available over northern Brazil during this period. Negative precipitation anomalies predominate over northern SESA, while positive anomalies, although weaker than those in Fig. 1a, occurred in the southern region (northeastern Argentina and Uruguay). In Fig. 1d, the warmer SST anomalies observed over the Equatorial Pacific are weaker, and the maximum anomaly is displaced westward when compared with Fig. 1b. Over the subtropical Pacific Ocean, slightly negative SST anomalies are found in both hemispheres. Positive SST anomalies are observed over equatorial Atlantic Ocean close to the South American continent. Some previous studies have identified an equatorial zonal Atlantic mode with more intense SST anomalies displaced eastward compared to the SST pattern observed in Fig. 1d over the same region (Servain 1991; Zebiak 1993). The equatorial zonal Atlantic mode peaks in austral summer, similar to ENSO, though with shorter duration (3 months) of warm/cold phases, and occurs on seasonal and interannual timescales with higher signal over the subtropics. During the warm phase of the equatorial zonal Atlantic mode, the SST anomalies over the equatorial Atlantic are slightly above normal inducing a reduction in SLP and weakening of the trade winds. During the cold phase of the Atlantic mode, opposite features are observed. The pattern found in Fig. 1d over the western Equatorial Atlantic characterized by positive SST anomalies has not previously been described in the literature, and further analysis must be performed.

The anomalous atmospheric circulation patterns related to the SST anomalies described above are shown in Fig. 2 during EN years for the PDO(+) (Fig. 2a–c) and PDO(−) (Fig. 2d–f) phases. Figure 2a shows the establishment of weak anticyclonic ψ(200 hPa) anomalies over the western part of South American tropics contributing to the ascending motion in this region (Fig. 2b). The anticyclonic circulation at upper levels over the SESA and Paraguay regions, although weak, may contribute to the secondary meridional circulation and consequently an increase in convection over the region according to Zhou and Lau (2001). The low level vertically integrated moisture flux and its divergence (Fig. 2c) show anomalous eastern moisture flux and divergence over the eastern equatorial Atlantic Ocean. A weak anomalous moisture flux convergence was observed over the central Amazon region followed by ascending motion over this region (Fig. 2b).

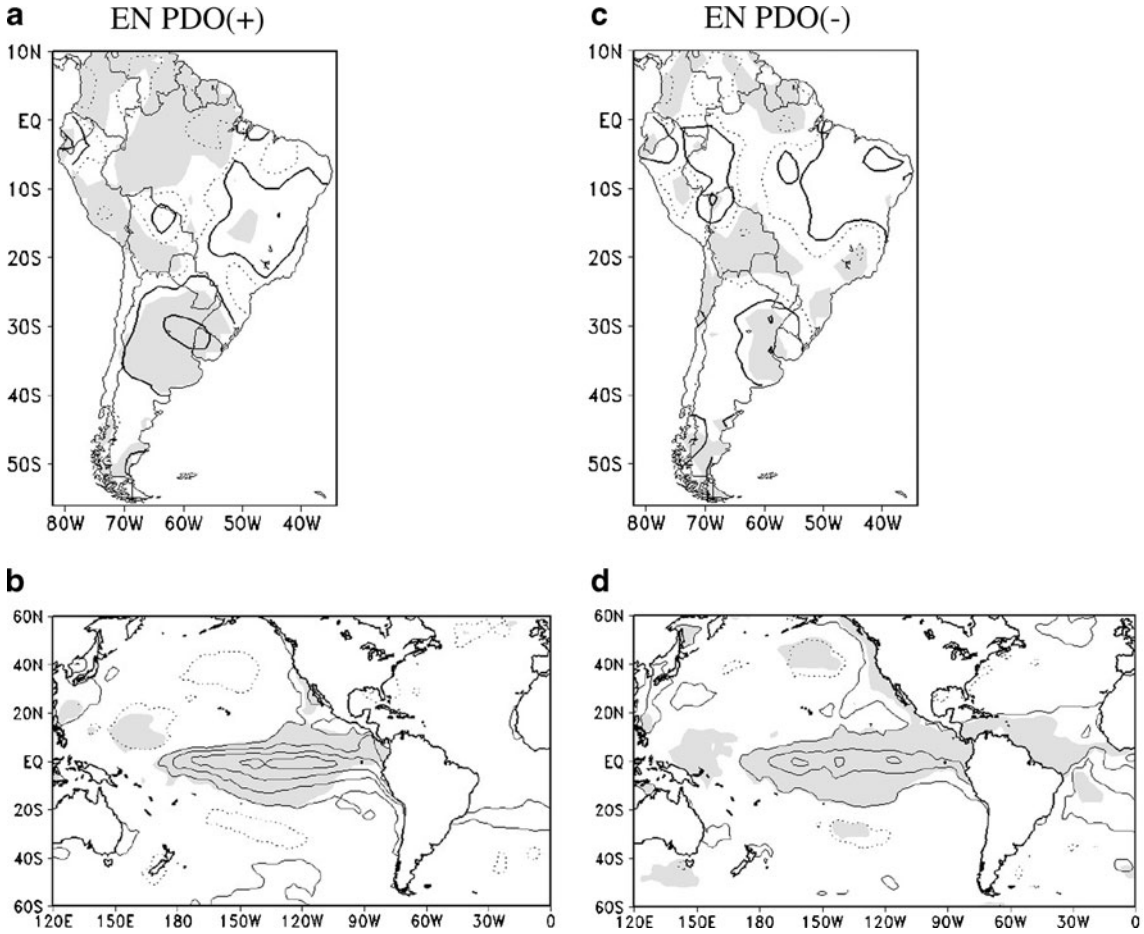

Fig. 1 Anomaly composites during austral summer of EN years for PDO(+) phase or El Niño-like: **a** Precipitation; **b** SST. **c**, **d** As in **a** and **b** but for PDO(−) phase or La Niña-like. Contour intervals are 3 mm day^{-1} and 0.4°C. Negative contours are *dotted*, and the zero contours are the *continuous line*. Areas where the anomalies are statistically significant according to a *t* test at 90% level are *shaded*

The slightly negative precipitation anomalies over northern part of continent are in accordance with the weak anticyclonic ψ(200 hPa) anomalies and weak anomalous moisture flux convergence mentioned previously over this region. Also, over the western Amazon, an anomalous moisture flux divergence is observed, whereas a northwesterly anomalous flux and anomalous moisture flux convergence prevailed over the SESA portion. Such pattern is coherent with the ascending motion resulting in the observed positive precipitation anomalies over the SESA region, as depicted in Fig. 1a.

During EN in the PDO(−) phase (Fig. 2c), the 200-hPa anomalous anticyclone over the Pacific was 30º westward displaced compared to its position in Fig. 2a. The associated PSA wave train (Karoly 1989; Mo and Paegle 2001) extends from the central-east Pacific returning to the north near 60ºS reaching tropical latitudes over the Atlantic Ocean (Fig. 2d). Cyclonic anomalies predominate over most of South America, but they are more pronounced over the tropics where there is an anomalous descending motion over the north and northeast regions (Fig. 2e). Around 40°S, the gradient between the weak cyclonic anomalies and the anticyclonic anomalies over southern Brazil and Uruguay contributes to the intensification of the westerly winds. In Fig. 2f, a weak anomalous moisture divergence over the western equatorial Atlantic and an anomalous moisture flux divergence with anticyclonic curvature over central-southeastern Brazil may have contributed to the weakening of the easterly trade winds over the region. The weakening of the trade winds is also favored by the positive anomalous SST in equatorial Atlantic Ocean (Fig. 1d) and consequent reduction in SLP over the region. The west branch of this anticyclonic circulation contributes to the intense anomalous meridional moisture flux from Amazon toward southern Brazil, suggesting that the moisture availability from the equatorial Atlantic is more important in generating intense positive precipitation anomalies over the SESA region than the moisture flux from the Amazon region. This circulation pattern is similar to those found by Herdies et al. (2002) and Drumond and Ambrizzi (2005). According to these authors,

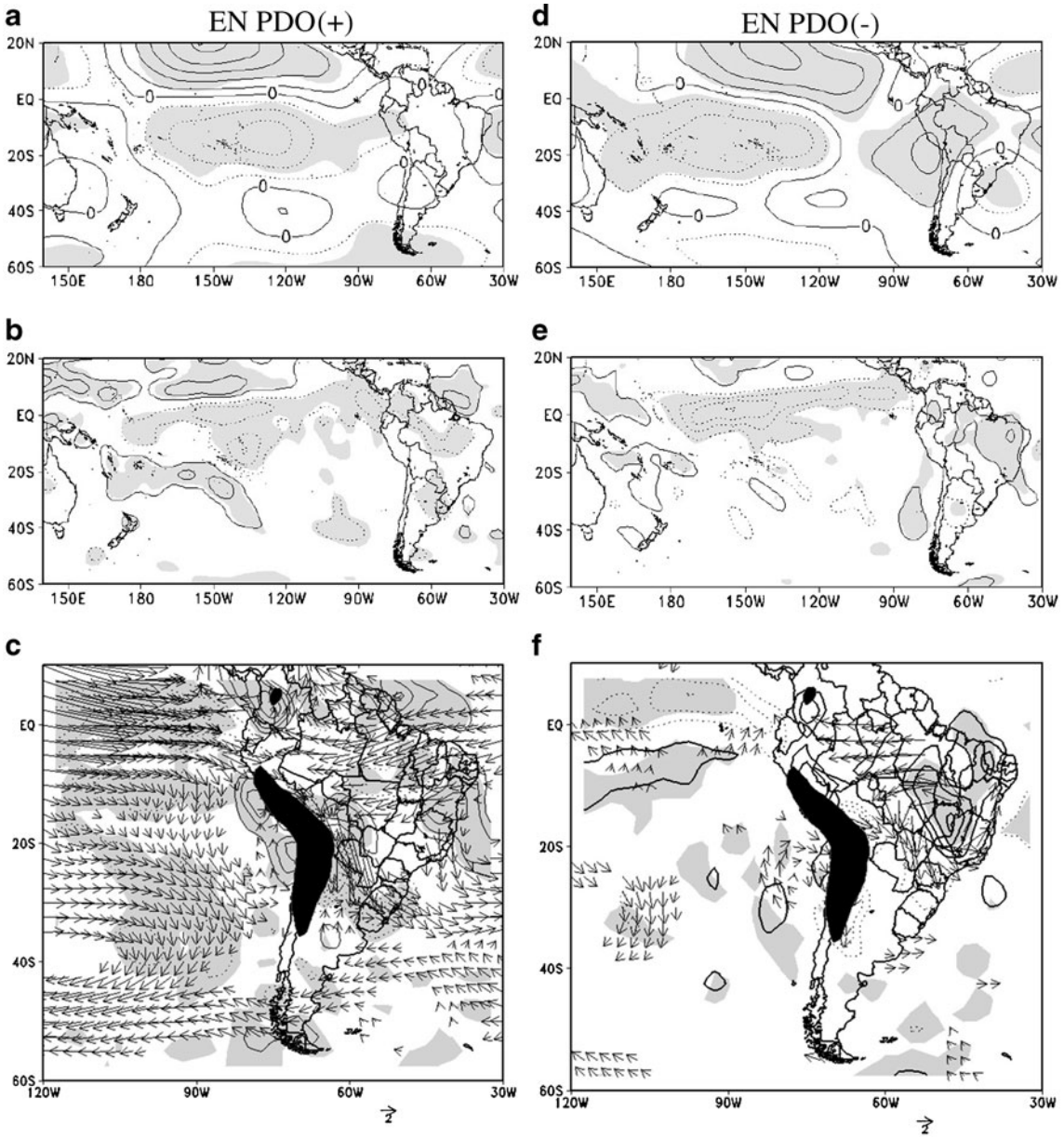

Fig. 2 Anomaly composites during austral summer of EN years for the PDO(+): **a** Zonally asymmetric 200-hPa streamfunction—ψ; **b** 500-hPa Omega—ω; **c** Vertically integrated moisture flux (g kg^{-1} m s^{-1}) and its divergence between 1,000 and 850 hPa. **d**, **e**, **f** As in **a**, **b**, and **c** but for the PDO(−). Contour intervals are 2×10^6 $m^2 s^{-1}$, 1 $hPas^{-1}$, and 1 mm day^{-1}, respectively. Negative contours are *dotted*, and the zero contours are the *continuous line*. Areas where the anomalies are statistically significant at 90% level are *shaded*

the weakening of the moisture transport toward the South Atlantic Convergence Zone (SACZ) was due to a shifting of moisture transport from the Amazon toward southern Brazil, contributing to the positive precipitation anomalies in this region. In fact, this pattern seems to favor the negative precipitation anomalies (Fig. 1c) over northern SESA, a region which is usually affected by Oceanic SACZ as mentioned in Carvalho et al. (2004). Over southern SESA, the positive precipitation anomalies shown in Fig. 1c were less intense than in Fig. 1a. This is consistent with a weaker moisture flux from the Amazon basin toward this region (Fig. 2f). In order to investigate some possible influence of cyclogeneses over the precipitation anomalies, an analysis of properties of extratropical cyclones is shown in Fig. 3.

Figure 3 shows properties of the extratropical cyclone activity (SD and CP) over South America during EN years in the PDO(+) (Fig. 3a, b) and PDO(−) (Fig. 3c, d) phases. The SD anomalous pattern in Fig. 3a is slightly above normal over two regions: (1) in the extreme southern Brazil, northeastern Argentina, Uruguay, and in the vicinity on the southwestern Atlantic Ocean, and (2) over the San Matías Gulf, in the Southwest Atlantic Ocean. According to

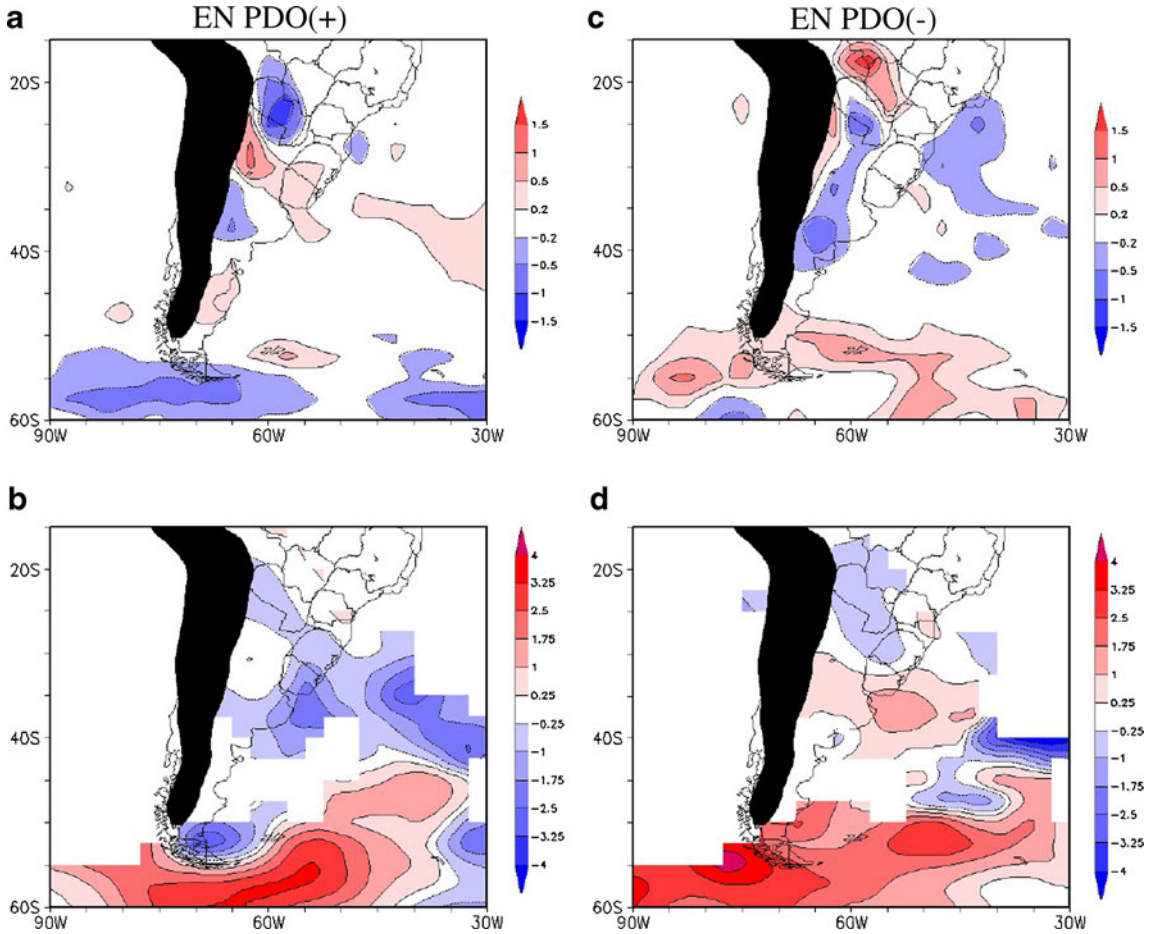

Fig. 3 **a** System Density (SD) and **b** Central Pressure (CP) anomalies of cyclogeneses during the austral summer of EN events for the PDO (+) phase. **c**, **d** The same as in **a** and **b** but for EN years during the PDO(−) phase. Only systems with a lifetime above 24 h were considered. The contour intervals are 0.5 cyclones/(deg. lat)^2 and 1.5 hPa

Gan and Rao (1991), both of these locations are favorable for cyclogeneses. In fact, as seen in Fig. 2c, the SESA region was influenced by significant anomalous moisture convergence originating from the tropics. This situation contributes to SLP reduction, and as mentioned by Berbery and Barros (2002) and Magaña and Ambrizzi (2005), it can favor cyclogeneses in these regions. Figure 3b shows anomalous negative CP (more intense cyclones than normal) over a large part of the domain with the exception of the region around 60ºS. Over the San Matías Gulf, there are no significant values. Both positive SD and negative CP anomalous patterns mentioned earlier seem to contribute for the positive precipitation anomalies over SESA region observed in Fig. 1a. In contrast with Fig. 3a, Fig. 3c shows negative SD anomalies over northeastern Argentina, part of southern Brazil, and the subtropical Atlantic Ocean. This negative SD pattern is consistent with less availability of humidity over these areas as observed in Fig. 2f when compared with Fig. 2c. Positive CP anomalies were also observed over most of these regions (Fig. 3d) indicating weaker cyclones when compared to Fig. 3b. The negative precipitation anomalies over northern SESA and the positive ones on southern region (but less intense than those in Fig. 1a) are in accordance with the negative SD and positive CP anomalous patterns described during EN events for the PDO(−).

The previous analyses presented in this study indicate that extratropical cyclones detected over most of southern South America and neighboring Atlantic Ocean were more frequent and more intense during PDO(+) years than during PDO(−) years. These analyses agree with Pezza et al. (2007), although these authors used a different methodology and different observational data to the dataset we used here (the ERA40 reanalysis data). It should be emphasized that a detailed analysis of regional moisture transport and atmospheric circulation anomalies over the key areas was not explored by the earlier authors. The present results suggest that the main mechanism responsible for the increase in density and deepening of extratropical cyclones properties over most of southern South America and

neighboring Atlantic Ocean seems to be related to a larger transport of tropical warm moisture by the SALLJ toward these regions during PDO(+) compared to PDO(−) years.

In summary, there are significant differences between SST and atmospheric circulation anomalies during austral summer of EN events for opposite PDO phases that can be linked to differences in planetary waves originating in the equatorial Pacific. During PDO(+) phase of 1977–1999, EN events were associated with anomalous warm water displaced eastward over the equatorial Pacific when compared to the events that occurred between 1950 and 1976 (a cold/PDO(−) phase). These events were followed by a slight warming in the western equatorial Atlantic that was not there during PDO(+) phase. Such differences in anomalous SST behavior seem to contribute to the differences in atmospheric wave patterns at upper levels. Consequently, changes in anomalous tropic–extratropic circulation can affect the moisture regime over the continent, particularly over the SESA region. This result agrees with Ambrizzi et al. (2004) in some aspects. They observed that not all EN events produce a canonical impact, and that a joint influence of the equatorial Pacific and tropical Atlantic can modulate the circulation cells and the associated precipitation regime. In the next section, the numerical experiments will be used to further investigate these issues.

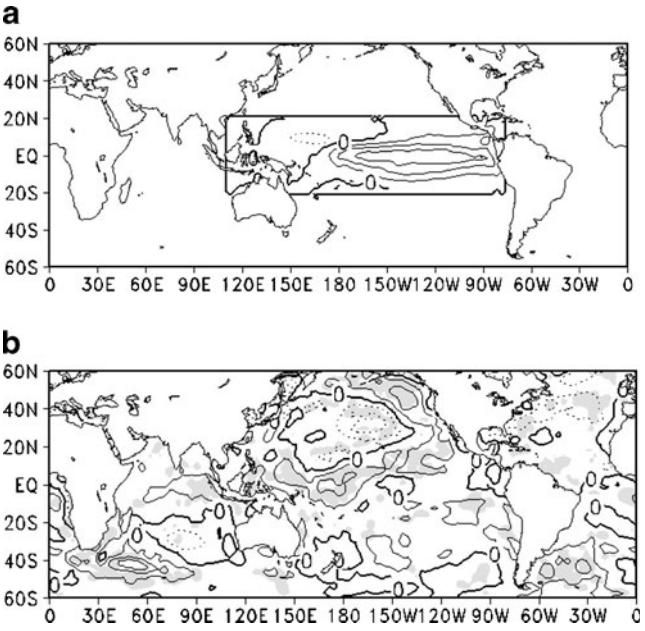

Fig. 4 **a** Canonical anomalous equatorial forcing in the *box* 20ºS–20ºN;120ºW–175ºW used in ENPDO(+) and ENPDO(−) numerical experiments. **b** Difference of mean SST prescribed globally in ENPDO(+) minus the ENPDO(−). See Section 2.2.2 for more details. Contour intervals are 0.4°C, and zero contours are in *bold*. Negative contours are *dotted*. The *shaded* in **b** indicates areas where the difference between the mean SST for the PDO(+) and PDO(−) phase is statistically significant at the 90% level of a two-tailed *t* test assuming 1° of freedom per event

3.2 Summertime South American atmospheric circulation, El Niño, and PDO: numerical experiments

How could the phase of the PDO affect the EN teleconnections toward South America? In other words, we wonder whether there is or no impacts of SST anomalies of a "canonical" EN change in the presence of PDO(+) and PDO(−) global SST and sea ice conditions. In order to answer these questions, two numerical experiments were conducted following the design presented in Section 2.2.2 and Table 2.

The anomalous equatorial forcing for DJF season used in both ENPDO(+) and ENPDO(−) numerical experiments is showing in Fig. 4a. According to Fig. 4a, the more intense positive SST anomalies are positioned over central eastern Pacific Ocean similar to those in canonical EN events. The mean difference between the globally SST climatology used in ENPDO(+) and ENPDO(−) experiments for the DJF season is illustrated in Fig. 4b. Positive differences are positioned over the South Atlantic Ocean mainly over the southwestern basin with maximum statistical significant between 10–60ºW;30–60ºS. Such differences indicate more intense SST values during PDO(+) compared to PDO(−) over these regions. Over subtropical latitudes over the most of North Pacific and North Atlantic Oceans, the negative differences indicate less intense SST values during PDO(+) compared to PDO(−) over this regions. Positive and significant SST differences are found over North Pacific, Western Equatorial Pacific, and most of South Pacific. The differences found over the southern Indian Ocean between 10–90ºE;35–50ºS and near the Sumatra Coast are similar to SST anomalies found by Chan et al. (2008) and Drumond and Ambrizzi (2005). These authors show that positive anomalies near the southeastern Africa and negative eastward contribute with dry conditions over SACZ region and increase in summer precipitation over the South America subtropics. Such precipitation pattern is accompanied by a wave train similar to PSA emanating from south Indian Ocean toward the subtropical South American continent (e.g., Saji et al. 2005).

Figure 5 shows the difference between ENPDO(+) minus the ENPDO(−) experiments. For precipitation, the most pronounced difference is located on northern continent with negative values, besides a meridional dipole with positive difference on eastern tropical Brazil and negative values over most of Southeast Brazil (Fig. 5a). Such differences indicate a more intense precipitation regime on northern continent and most of Southeast Brazil during the canonical EN during PDO(−) compared to those in PDO(+) EN. However, the opposite seems to occur in eastern tropical Brazil. The difference in 200 hPa streamfunction

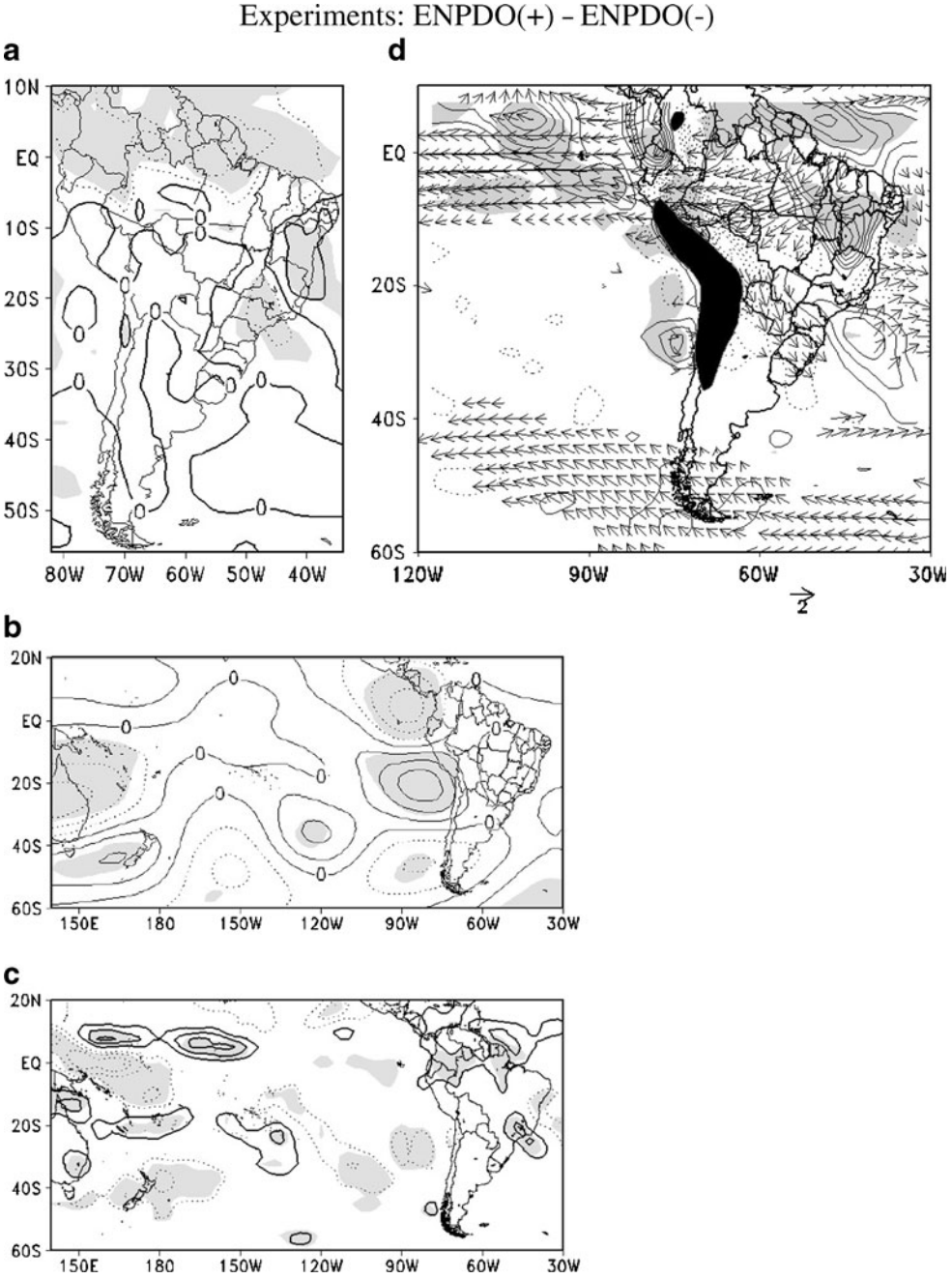

Fig. 5 Difference between the ensemble of the ENPDO(+) and ENPDO(−) numerical experiments. **a** Precipitation; **b** Zonally asymmetric 200-hPa streamfunction—ψ; **c** 500-hPa Omega—ω; and **d** Vertically integrated moisture flux (g kg^{-1} m s^{-1}) and its divergence between 1,000 and 850 hPa. Contours intervals are 1 mm day^{-1}, 2×10^6 m^2s^{-1}, 1 $hPas^{-1}$, and 0.5 mm day^{-1}, respectively. Negative contours are *dotted*, and the zero contours are exhibited as *continuous line*. The *shaded* indicates areas where the difference between two mean of the numerical experiments is statistically significant at the 90% level of a two-tailed *t* test assuming 1° of freedom per event

(Fig. 5b) shows a weak wave train pattern which is probably related to the precipitation differences observed in Fig. 5a. Figure 5c shows that the positive differences in ω(500 hPa) are simulated over northern South America in the vicinity of Atlantic Ocean between 0 and 15°N, most of Southeast Brazil and in the vicinity of the Southwestern Atlantic Ocean. These positive differences seem to be associated with more intense ascending motion over these regions during PDO(−) compared to PDO(+), which could explain the negative precipitation differences in Fig. 5a. The negative differences in the ω(500 hPa) field simulated over eastern tropical Brazil suggest more intense descending motion during PDO(−) compared to PDO(+) in accordance with Fig. 5a. Figure 5d shows that the positive differences in the low level integrated moisture flux and its divergence are associated with an anticyclonic circulation on the northeastern continent and equatorial Atlantic Ocean. Such differences are in agreement with the positive difference in ω(500 hPa) field shown in Fig. 5c and the negative difference in precipitation shown in Fig. 5a. Over most of Southeast Brazil and vicinity Southwest Atlantic Ocean, the positive difference is associated with cyclonic convergence toward eastern tropical Brazil. This seems to be in accordance with the maximum SST warming over the

Southwestern Atlantic Ocean during PDO(+) compared to PDO(−) as shown in Fig. 4b. The warming may contributes with the reduction in SLP and southwestward weakening of the South Atlantic High, which could explain the simulated difference in the most of Southeast Brazil shown in Fig. 5a. However, this is just a speculation. Additional numerical experiments isolating the observed variability of SST over several oceanic basins during different PDO phases shown in Fig. 4b will be conducted in order to verify this possibility

4 Summary and concluding remarks

Recent studies have shown that seasonal precipitation cycle over the South American continent is modulated by ENSO and PDO (Andreoli and Kayano 2005; Garcia and Kayano 2006; Kayano and Andreoli 2007). However, some important questions have not yet been discussed in the literature in detail.

Our particular attention focused on the impact of EN events during positive PDO(+) and negative PDO(−) phases on transport of moisture and extratropical cyclonic properties in austral summer over South America, which was investigated in this work through an observational and numerical analysis. Based on the observational results, a conceptual diagram is presented in Fig. 6. The green arrows represent the meridional moisture flux from the tropics to the extratropics. The weaker SST, precipitation (Prec), and atmospheric circulation anomalies during PDO(−) are represented by light colors compared with the more intense anomalies during PDO(+) which are represented by dark colors. This figure suggests that the changes in tropical–extratropical circulation anomalies over South America after 1976 seem to be associated with an increase in the frequency and intensity of EN events. In Fig. 6a, for the EN events during PDO(+), the presence of negative precipitation anomalies over northern Amazon (yellow circle) and

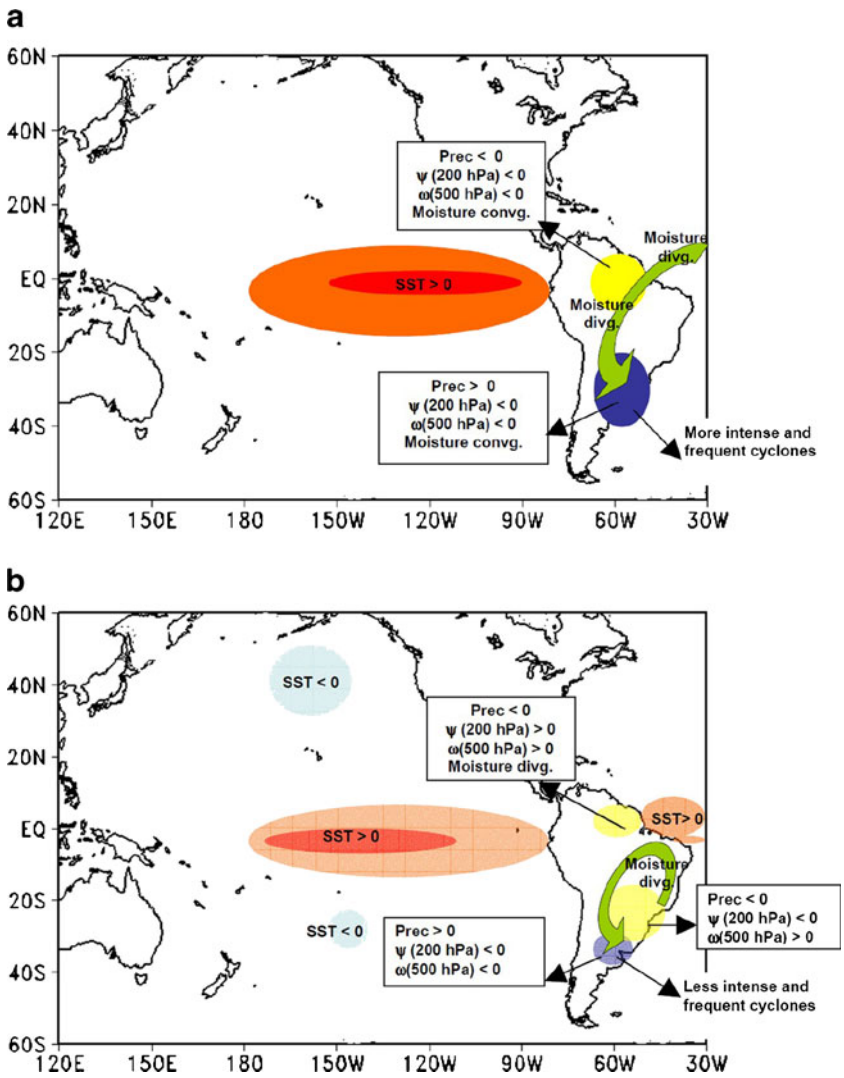

Fig. 6 Conceptual diagram of the observed anomalies obtained from the observational and numerical results during EN events for **a** PDO(+) and **b** PDO(−) phases. The *green arrows* represent the meridional moisture flux from the tropics to the extratropics. The weaker *SST*, precipitation (*Prec*), and atmospheric circulation anomalies occurred during PDO(−) are represented by *light colors* compared to the more intense anomalies occurred during PDO (+) represented by *dark colors*

positive anomalies over most of southeastern South America (SESA) (blue circle) are associated with intense positive SST anomalies over equatorial Pacific presenting maximum values in eastern basin (red circle). The related zonally asymmetric streamfunction anomaly at 200 hPa exhibits anticyclonic anomalies over most part of the continent with the exception of northeast Brazil, where cyclonic anomalies prevail. This pattern can favor ascending motion over the Amazon and SESA regions. The vertically integrated moisture flux and its divergence at lower levels showed divergence in the western equatorial Atlantic and convergence over the Amazon region. This is consistent with vertical ascending movement observed over this area, which helps to maintain the anticyclonic circulation over the tropics at upper levels. Nevertheless, some anomalous moisture flux divergence is observed over the western Amazon followed by a northwesterly anomalous flux and anomalous moisture flux convergence over the SESA portion. This pattern seems to contribute with the above normal extratropical cyclone density and below normal central pressure over this region.

For the EN events during PDO(−) (Fig. 6b), precipitation tends to be above normal in southern SESA region but less intense than in Fig. 6a over this region (light blue circle), and below normal northward (light yellow circle). These anomalies are associated with positive SST anomalies over the equatorial Atlantic Ocean close to the South American coast, and with a slight warming in the central equatorial Pacific Ocean that shows less intense SST anomalies compared with Fig. 2a (light red circle). The SST anomalous pattern described over the equatorial Atlantic Ocean induces a reduction in SLP and consequently a weakening of the easterly trade winds over this region as observed in Fig. 2f. The associated PSA wave train configured in response to the warming in SST over central equatorial Pacific Ocean contributes with cyclonic anomalies over the tropics on the continent. Such anomalous pattern seems to influence downward motion and anomalous divergence over central eastern Brazil followed by a weakening of the moisture flux from equatorial Atlantic and reduction of the moisture availability toward the SESA region. The extratropical cyclones tend to be weaker and less frequent over most of Southern SESA, and they also show weaker central pressure when compared to the situation during PDO(+) EN.

The observational composites suggested that the differences in response over South America to EN events observed during PDO(+) and PDO(−) phases can be related to differences in equatorial Pacific and Atlantic SST anomalies, which could trigger distinct teleconnection patterns. To complement the observational results, two numerical experiments were performed. The purpose was to investigate whether impacts of a canonical EN event over South America could change under different PDO climatology regimes. The numerical results suggested that the role of global SST and sea ice associated with different PDO phases seems to have played an important role in the difference of the canonical El Niño response over South America (Fig. 5). Through the differences in SST PDO climatologies (Fig. 4b), we speculate the importance of others oceanic basins besides the equatorial Pacific in modulating the South American summer circulation is speculated. This hypothesis is supported by some previous studies (e.g., Chan et al. 2008; Drumond and Ambrizzi 2005) that mentioned the importance on the impact of the SST anomalies over the Indian Ocean (similar to those shown in Fig. 4b) over the South American continent. However, additional numerical experiments are still necessary to investigate this possibility in detail.

This work contributes for a better understanding of the impact of atmosphere low frequency variability modes over South America. Additional numerical experiments are in progress to investigate the particular role of the changes observed in oceanic basins during the evolution of PDO over the impact of the evolution of a canonical El Niño over South American climate. Analysis considering data for future climate change scenarios has been carried out at the moment, and it will be presented elsewhere.

Acknowledgments We thank the editor and the constructive comments of the anonymous reviewers. We also thank M. Chen and collaborators for providing rainfall data and the Climate Prediction Center (CPC/NCEP/NWS) and UK Meteorological Office Hadley Centre for providing the datasets. This work was supported by "Fundação de Amparo à Pesquisa do Estado de São Paulo" (FAPESP 05/01804-0). AD acknowledges the support from FAPESP, from CNPq, and from the Spanish Ministry from Science and Innovation. TA acknowledges the partial support from CNPq/INCT of Climate Change, CAPES, and he has also received funding from the European Community's Seventh Framework Programme (FP7/2007-2013) under Grant Agreement No. 212492 (CLARIS LPB. A Europe-South America Network for Climate Change Assessment and Impact Studies in La Plata Basin).

References

Ambrizzi T, Souza EB, Pulwarty RS (2004) The Hadley and walker regional circulations and associated ENSO impacts on South American seasonal rainfall. In: Diaz HF, Bradley RS (eds) The Hadley circulation: present, past and future. Kluwer Publishers 7:203–235

Andreoli RV, Kayano MT (2005) ENSO-related rainfall anomalies in South America and associated circulation features during warm and cold Pacific Decadal Oscillation regimes. Int J Climatol 25:2017–2030. doi:10.1002/joc.1222

Berbery EH, Barros VR (2002) The hydrological cycle of the La Plata Basin in South America. J Hydrometeorol 3:630–645

Carvalho LMV, Jones C, Liebmann B (2004) The South Atlantic convergence zone: intensity, form, persistence, and relationships with intraseasonal to interannual activity and extreme rainfall. J Climate 17:88–108

Carvalho LMV, Jones C, Ambrizzi T (2005) Opposite phases of the Antarctic oscillation and relationships with intraseasonal to interannual activity in the tropics during the austral summer. J Climate 18:702–718. doi:10.1175/JCLI-3284.1

Chan S, Behera S, Yamagata T (2008) Indian Ocean dipole influence on South American rainfall. Geophys Res Lett 35(14):L14S12

Chen M, Xie P, Janowiak JE, Arkin EPA (2002) Global land precipitation: a 50-yr monthly analysis based on gauge observations. J Hydrometeorol 3(3):249–266

Collins WD, Rasch PJ, Boville BA, Hack JJ, Mccaa JR, Williamson DL, Briegleb B, Bitz C, Lin SJ, Zhang M (2006) The formulation and atmospheric simulation of the community atmosphere model: CAM3. J Climate 19(11):2144–2161. doi:10.1175/JCLI3760.1

Dettinger MD, Battisti DS, Garreaud RD Jr, Mccabe GJ, Bitz CM (2001) Interhemispheric effects of interannual and decadal ENSOlike climate variations on the Americas. In: Markgraf V (ed) Interhemispheric climate linkages. Academic, San Diego, pp 1–16

Douglas MW, Peña M, Villarpando R (2000) Special observations of the low level flow over eastern Bolivia during the1999 atmospheric mesoscale campaign. Extended Abstracts of the 6th International Conference on Southern Hemisphere Meteorology and Oceanography. Santiago, Chile

Drumond ARM, Ambrizzi T (2005) The role of SST on the South American atmospheric circulation during January, February and March 2001. Climate Dyn 24:781–791

Enfield DB, Mestas-Nuñez A (1999) Multiscale variabilities in global sea surface temperatures and their relationships with tropospheric climate patterns. J Climate 12:2719–2733

Folland CK, Renwick JA, Salinger MJ, Mullan AB (2002) Relative influences of the IPO and ENSO on the South Pacific convergence zone. Geophys Res Lett 29(13):10.1029

Gan MA, Rao VB (1991) Surface cyclogeneses over South America. Mon Weather Rev 119:1293–1302

Garcia SR, Kayano MT (2006) South American Monsoon during the two phases of The Pacific Decadal Oscillation. Proceedings of 8 ICSHMO 1049–1055. Foz do Iguaçu, Brazil

Herdies DL, Da Silva A, Silva Dias MA, Ferreira RN (2002) Moisture budget of the bimodal pattern of the summer circulation over South America. J Geophys Res 107:8075–8084

Kalnay E, Kanamitsu M, Kistler R, Collins W, Deaven D, Gandin L, Iredell M, Saha S, White G, Woollen J, Zhu Y, Chelliah M, Ebisuzaki W, Higgins W, Janoviak J, Mo KC, Ropelewski C, Wang J, Leetmaa A, Reynolds R, Roy J, Joseph D (1996) The NCEP/NCAR 40-year reanalysis project. Bull Am Meteorol Soc 77(3):437–471

Karoly DJ (1989) Southern hemisphere circulation features associated with El Niño–Southern Oscillation events. J Climate 2:1239–1252

Kayano MT, Andreoli RV (2007) Relations of South American summer rainfall interannual variations with the Pacific Decadal Oscillation. Int J Climatol 27:531–540

Kiladis GN, Mo KC (1998) Interannual and intraseasonal variability in the Southern Hemisphere. Meteorology of the Southern Hemisphere, Meteor Monogr 49, Amer Meteor Soc 307–336

Magaña V, Ambrizzi T (2005) Dynamics of subtropical vertical motions over the Americas during El Niño boreal winters. Atmósfera 18(4):211–233

Mantua NJ, Hare SR, Zhang Y, Wallace JM, Francis RCA (1997) Pacific interdecadal climate oscillation with impacts on salmon production. Bull Am Meteorol Soc 78:1069–1079

Marengo J (2004) Interdecadal and long term rainfall variability in the Amazon basin. Theor Appl Climatol 78:79–96

Marengo JA, Soares WR, Saulo C, Nicolini M (2004) Climatology of the Low-Level Jet east of the Andes as derived from the NCEP reanalyses. J Climate 17:2261–2280

Mendes D, Souza EP, Trigo IF, Miranda PMA (2007) On precursors of South American cyclogeneses. Tellus Ser A 59(1):114–121. doi:10.1111/j.1600-0870.2006.00215.x

Mo KC, Paegle JN (2001) The Pacific-South American modes and their downstream effects. Int J Climatol 21:1211–1229

Murray RJ, Simmonds I (1991a) A numerical scheme for tracking cyclone centers from digital data. Part I: development and operation of the scheme. Aust Meteorol Mag 39:155–166

Murray RJ, Simmonds I (1991b) A numerical scheme for tracking cyclone centres from digital data. Part II: application to January and July general circulation model simulations. Aust Meteorol Mag 39:167–180

Newman M, Compo GP, Alexander MA (2003) ENSO-forced variability of the Pacific decadal oscillation. J Climate 16:3853–3857

Oleson KW, Dai Y, Bonan GB, Bosilovich M, Dickinson R, Dirmeyer P, Hoffman F, Houser P, Levis S, Niu G-Y, Thornton P, Vertenstein M, Yang Z-L, Zeng X (2004) Technical description of the Community Land Model (CLM) Technical Report NCAR/TN-461+STR, National Center for Atmospheric Research, Boulder, CO. 80307–3000, p 174

Paegle J (1998) A comparative review of South American low level jets. Meteorologica 3:73–82

Parker DE, Folland CK, Jackson M (1995) Marine surface temperature: observed variations and data requirements. Clim Change 31:559–600

Pezza AB, Ambrizzi T (2003) Variability of southern hemisphere cyclone and anticyclone behavior: further analysis. J Climate 16 (7):1075–1083

Pezza A, Simmonds I, Renwick J (2007) Southern hemisphere cyclones and anticyclones: recent trends and links with decadal variability in the Pacific Ocean. Int J Climatol 27:1403–1419. doi:10.1002/joc.1477

Power S, Colman R (2006) Multi-year predictability in a coupled general circulation model. Climate Dyn 26:247–272

Power SB, Smith IN (2007) Weakening of the walker circulation and apparent dominance of El Niño both reach record levels, but has ENSO really changed? Geophys Res Lett 34:L18702. doi:10.1029/2007GL030854

Power S, Casey T, Folland C, Colman A, Mehta V (1999) Interdecadal modulation of the impact of ENSO on Australia. Climate Dyn 15:319–324

Power S, Haylock M, Colman R, Wang X (2006) The predictability of interdecadal changes in ENSO activity and ENSO teleconnections. J Climate 19:4755–4771

Rayner NA, Parker DE, Horton EB, Folland CK, Alexander LV, Rowell DP, Kent EC, Kaplan A (2003) Global analyses of sea surface temperature, sea ice, and night marine air temperature since the late nineteenth century. J Geophys Res 108(D14):4407. doi:10.1029/2002JD002670

Reboita MS; Ambrizzi T; da Rocha RP (2009) Relationship between the southern annular mode and southern hemisphere atmospheric systems. Brazilian Journal of Meteorology 24(1). doi:10.1590/S0102-77862009000100005

Robertson AW, Mechoso CR (2000) Interannual and interdecadal variability of the South Atlantic convergence zone. Mon Weather Rev 128:2947–2957

Saji NH, Ambrizzi T, Ferraz SET (2005) Indian Ocean Dipole events and austral surface air temperature anomalies. Dyn Atmos Ocean 39:87–101

Saulo AC, Nicolini M, Chou SC (2000) Model characterization of the South American low-level flow during the 1997–1998 spring–summer season. Clim Dyn 16:867–881

Schneider N (2005) The forcing of the pacific decadal oscillation. J Clim 18:4355–4373. doi:10.1175/JCLI3527.1

Servain J (1991) Simple climatic indices for the tropical Atlantic Ocean and some applications. J Geophys Res 96:15137–15146

Silva GAM, Ambrizzi T (2006) Inter-El Niño variability and its impact on the South American low-level jet east of the Andes during austral summer—two case studies. Advans Geosci 6:283–287, SRef-ID: 1680- 7359/adgeo/2006-6-283

Silva GAM, Ambrizzi T (2009) Summertime moisture transport over Southeastern South America and extratropical cyclones behavior during inter-El Niño events. Theor Appl Climatol. doi:10.1007/s00704-009-0218-6

Silva GAM, Ambrizzi T, Marengo JA (2009) Observational evidences on the modulation of the South American Low Level Jet east of the Andes according the ENSO variability. Ann Geophyc 27:645–665

Silvestri G (2004) El Niño signal variability in the precipitation over southeastern South America during austral summer. Geophys Res Lett 31:L18206. doi:10.1029=2004GL020590

Smith TM, Reynolds RW, Livezey RE, Stokes DC (1996) Reconstruction of historical sea surface temperatures using empirical orthogonal functions. J Climate 9:1403–1420

Vera C, Silvestri G, Barros V, Carril A (2004) Differences in El Niño response over the Southern Hemisphere. J Climate 17:1741–1753

Wilks DS (1995) Statistical methods in the atmospheric sciences. Academic, NY, p 468

Zebiak SE (1993) Air-sea interactions in the equatorial Atlantic region. J Climate 6:1567–1586

Zhang Y, Wallace JM, Battisti D (1997) ENSO-like interdecadal variability: 1900–93. J Climate 10:1004–1020

Zhou J, Lau KM (2001) Principal modes of interannual and decadal variability of summer rainfall over South America. Int J Climatol 21:1623–1644. doi:10.1002/joc.700

Zhou YP, Higgins RW, Kim H-K (2001) Relationships between El Niño-Southern Oscillation and the Arctic Oscillation: a Climate-Weather Link. NCEP/Climate Prediction Center Atlas 8 [Available online at http://www.cpc.ncep.noaa.gov/products/outreach/atlas.shtml]